

## Ricochet of Spheres on Sand of Various Temperature

Yoon Keon Kim\* and Woo Chun Choi#

*Department of Mechanical Engineering, Korea University, Korea*

*\*E-mail: gokkolove@korea.ac.kr*

### ABSTRACT

The debris generated by the explosion of a building or ammunition is flown far away through the ricochet phenomenon. The debris contains a very large amount of energy, and a risk factor surrounding it may be applied. The safety distance from debris is set from experiments or FEM analysis. The ricochet of debris is affected not only by the initial conditions of the debris, but also by the conditions of the medium. In this paper, the effect of sand temperature on the ricochet of sphere projectiles was investigated through experiments and FEM, by measuring the shear stress and internal friction angle when the sand temperature increases. As the temperature of the sand increases, the shear stress and the internal friction angle decrease, and the penetration depth of the projectile increases. As the depth of penetration becomes longer, the kinetic energy is lost more by the friction force with the sand and, the sphere projectile speed decreases more. This is mainly caused by the energy loss of the projectile, so the kinetic energy of the ricocheted projectile is reduced. Therefore, when setting the optimized inhabited building distance (IBD), the conditions of the medium should be taken into account.

**Keywords:** Ricochet; Debris; Shear stress; Internal frictional angle; Safety distance

### 1. INTRODUCTION

When buildings or ammunition magazines explode, steel and concrete debris is formed at the blasting sites, where most of the debris is flown away by the explosion energy. After colliding with the ground, some debris may be embedded in the ground, and other debris may ricochet or roll on the ground. The kinetic energy of the rebounded debris is very high, and can significantly damage people, buildings, and objects far away. The inhabited building distance (IBD) is defined as the minimum safety distance between the potential explosion site (PES) and the residential area, and is set for safety from dangerous debris. The IBD is determined as the distance to the final position of the ricocheted debris and the rolling debris through actual explosion test of magazines. The IBD depends on many factors, such as the size of the explosive debris, the mass of the explosive, the velocity of the debris, etc.

When the debris penetrates into a medium, the penetration depth and behaviour are changed, depending on the type and condition of the medium. This also affects the ricochet phenomenon<sup>1</sup>. The debris behaviour after impact with the medium varies with the type and condition of the medium. The reflection velocity and angle of the debris are changed. This means that the IBD may be longer or shorter, depending on the medium. For accurate IBD analysis, various types and conditions of the medium should be modeled in the FEM analysis program. Therefore, for proper modeling, it is necessary to investigate what characteristics change when the

type and condition of medium are changed through ricochet experiment of projectiles, and how these affect the behaviour of the projectile.

Water is the medium that was first used in the ricochet phenomenon. The ricochet phenomenon was used in naval battles in the 16<sup>th</sup> and 17<sup>th</sup> centuries in England, and during the World War II, it was famously used to destroy a dam. The critical angle of a projectile was measured in experiments, and some formulae were established to predict the critical angle of projectile. The critical angle of a spinning projectile was also investigated<sup>2,3,4</sup>.

Since a solid medium is present in a wide variety of conditions, ricochet onto a solid medium is more complicated than that onto water, and shows different tendency from that onto water. When the projectile ricochets onto sand, the critical angle of the projectile decreases as the velocity of the projectile increases. Conversely, when the projectile ricochets onto water, the critical angle increases as the velocity of the projectile increases<sup>5</sup>. To explain this, a ricochet model was developed that took into account the weight of a sphere projectile, and the static resistance of the medium in which penetration occurred. This model can predict the projectile behaviour when the collision angle is high, and the velocity of the projectile undergoes a significant change<sup>6</sup>. Also, when the spherical projectile penetrates through clay, the projectile trajectory depends on the surface pressure<sup>7</sup>. When a hardened steel sphere collides with ductile mild steel, the crater volume and the energy loss of the projectile were investigated according to the collision angle and velocity, and thus when oblique impact is applied, the rebound velocity could be measured very accurately.

A similar ricochet model predicted the exact crater dimensions and the volume, assuming constant dynamic yield pressure and friction coefficient<sup>8</sup>. A study of the ricochet of debris from the building explosion was also conducted. Cube projectiles were used besides sphere projectiles, and the projectile material was concrete. Various media were widely used, such as concrete, sand, water, and different clay<sup>9</sup>. Numerical study has shown that when a debris of different shape ricochets onto sand, the ricochet behaviour of debris changes with the internal friction angle of the sand<sup>10</sup>. Also, the shape and size of the debris affects the ricochet phenomenon<sup>11</sup>. Depending on the shape and material of the debris, the flight trajectory changes. This is because the drag and lift forces differ depending on the shape of the debris. Especially, the drag force affects the flight of the debris. In order to determine the total flying distance of the debris through the analysis, the drag and lift coefficients and the ricochet effect should be considered for the debris having a low incident angle<sup>12</sup>.

In this paper, the ricochet phenomenon of debris was studied according to the condition of the medium, not the type of medium. If the conditions change, even the same medium may have different properties<sup>13,14</sup>. Sand was selected as the medium. When the atmospheric temperature changes, the sand temperature changes. To change the conditions of the sand, the sand temperature was varied. In particular, in the desert region, the temperature fluctuation of the sand is large, because the daily temperature range is huge. A sphere was selected as the debris shape. In particular, the depth of the immersed edge is very important in the ricochet of spherical projectiles. The depth of the immersed edge of the projectile is related to the immersed area of the projectile, which is related to the energy dissipation that is associated with the ricochet<sup>1</sup>.

However, it is very difficult to measure the depth of the immersed edge in ricochet test. Thus, the penetration depth was measured through the vertical launch test according to the sand temperature. The penetration depth of the projectile depends on the sand resistance changes. In order to measure the sand resistance in this study, shear stress was measured by a direct shear test. Through the shear stress graphs in accordance with the sand temperature obtained by the direct shear test, the change of internal friction angle for each sand temperature was determined. The internal friction angles were applied to the sand material of the FEM analysis program, and the FEM was carried out, in which the effects of the internal friction angle were studied. Finally, the ricochet experiment was done on the sphere projectile in accordance with the sand temperature. The effects of sand temperature, shear stress, and internal friction angle on the penetration depth of projectile and ricochet of spherical projectile were investigated.

## 2. RICOCHET

In this study, Lydéric Bocquet's theory was used to study the ricochet phenomenon<sup>1</sup>. When a projectile collides with a medium, impact force is generated in the horizontal and vertical directions, according to the incident angle and velocity. When colliding with the medium, this impact force generates a drag force in accordance with the incident angle and velocity. When the drag is larger than the sum of the weight of the projectile

and the inertia force, it is bounced. This is called the ricochet phenomenon. Figure 1 shows a schematic of the impact process. The ricochet can be expressed as Eqn (1):

$$\vec{F} = \frac{1}{2} C_l \rho_w V^2 S_{im} \vec{n} + \frac{1}{2} C_f \rho_w V^2 S_{im} \vec{t} \quad (1)$$

where  $C_l$  is the lift coefficient,  $C_f$  is the tangential friction coefficient,  $\rho_w$  is the mass density of the medium,  $v$  is the speed of the projectile,  $S_{im}$  is the immersed area,  $\vec{n}$  is a unit vector perpendicular to the projectile, and  $\vec{t}$  is a vector parallel to the projectile<sup>1</sup>. Equation (1) is the force acting when the projectile penetrates into the medium. The immersed area depends on the shape of the projectile. The immersed area of the spherical projectile is expressed as Eqn. (2):

$$S_{im}(s) = R^2 [\arccos(1-s/R) - (1-s/R)\sqrt{1-(1-s/R)^2}] \quad (2)$$

where  $s = z/\sin\theta$  is the maximum immersed length, and  $z$  is the depth of the immersed edge of the projectile<sup>1</sup>. The penetration depth in the direction perpendicular to the surface of the medium.  $R$  is the radius of the spherical projectile. When  $R$  is constant, the maximum immersed length changes the behaviour of the projectile after the ricochet, which is related to the depth of the immersed edge of the projectile. The larger the surface area, the greater the energy loss of the projectile. In this study, the factors affecting the depth of the immersed edge of a projectile were investigated in accordance with the sand temperature, and the ways in which they affect ricochet were examined.

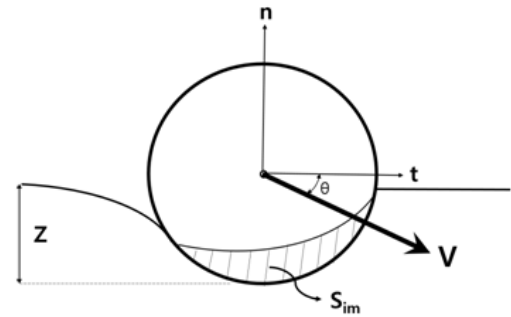


Figure 1. Schematic view of the impact process of a sphere projectile.

## 3. THE EXPERIMENTAL SET-UP

Two simple experiments were carried out prior to the ricochet experiment of the sphere projectile according to the sand temperature. The first experiment was to measure the shear stress according to the temperature change of the sand through a direct shear test, because when the projectile penetrates or ricochets onto the sand, the shear resistance is an important factor, and the shape of the graph shows the change in the internal friction angle of the sand. The second experiment was to measure the penetration depth of the projectile according to the temperature change of the sand, when the projectile was launched perpendicular to the sand. The penetration depth is an important factor related to sand resistance. It is very difficult to measure the penetration depth of a projectile in the ricochet experiment. Therefore, the penetration depth due to the

temperature effect can be visually obtained through the vertical launch test. Through the two experiments, the behaviour of the projectile can be predicted and compared according to the sand temperature. Finally, the behaviour of the projectiles after the ricochet was experimentally investigated according to the change of the sand temperature

**3.1 Direct Shear Test of the Sand Medium**

In this study, a direct shear test was performed to obtain the mechanical property for different sand temperatures. The shear resistance of sand is a result of friction and interlocking of particles, and possibly cementation or bonding at particle contacts. This may affect the penetration of a projectile. Figure 2 shows a direct shear-test-arrangement apparatus<sup>15</sup>. The sand was placed in a brass box, and the upper box could move horizontally. A normal force of 1 kg/cm<sup>2</sup> was applied through the loading plate. The shear stress was measured according to the failure of the sand specimen that was caused by the movement of the upper box.

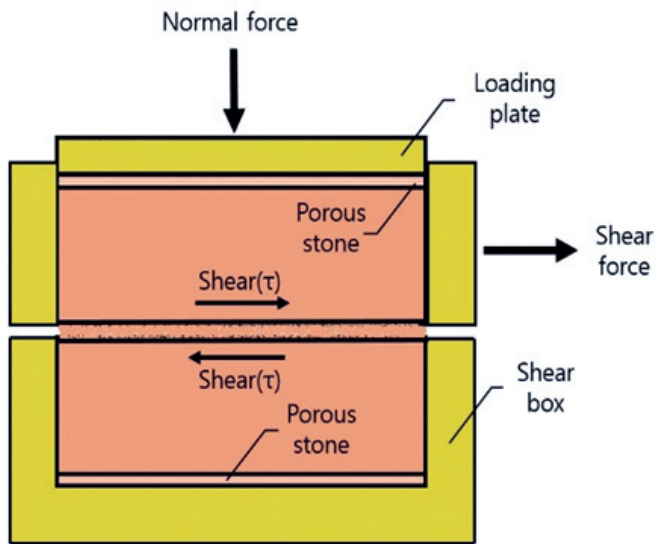


Figure 2. Direct shear-test arrangement.

A direct shear test was conducted to obtain the shear strength at sand temperatures of 20 °C, 50 °C, and 100 °C. The reason for selecting three temperatures was that the room temperature of the laboratory is 20 °C, while 50 °C is the normal daytime temperature of desert area<sup>16</sup>. Finally, 100 °C indicates when the temperature of the sand is extremely hot. The internal friction angle of the sand can be obtained by obtaining the shear stress diagram of the sand according to the temperature.

**3.2 The Test Set-up and the Equipment**

To perform the ricochet experiment and the penetration depth experiment of a sphere projectile according to the change in sand temperature, some equipment was used in the study. In previous researches, many methods have been used to launch spherical projectiles<sup>9,17</sup>. In this experiment, launching equipment was constructed by directly hitting spherical projectiles. The launching device used an air tacker that operates through an air compressor. The air tacker activates the pin by large air

pressure, and the pin hits the projectile and launches it. The incident velocity of the projectile can be controlled by varying the pressure of the air compressor. The maximum pressure of the air compressor is 7 bar, and the pressure used in the experiment is (4 bar, 5 bar, and 6 bar). When a steel sphere projectile is discharged at the three pressures, the projectile velocities are about (24 m/s, 28 m/s, and 32 m/s). The incident angles of the projectiles are (15 °, 20 °, and 25 °). The range of angles was determined through preceding research. When the incident angle is 25°, the (7 mm, 8 mm, and 10 mm) steel sphere does not ricochet from the velocity range of (24 m/s – 32 m/s).

This means that when a (7 mm, 8 mm, and 10 mm) steel ball impacts the sand, the critical angle is about 25°. Other necessary items are a box for holding the medium, and a high-speed camera for recording the trajectory of the projectile. The sand box dimensions are 270 mm × 170 mm × 60 mm. A 600 fps high-speed camera was used to record the path of the projectile. The incident velocity, reflection velocity, and reflection angle were calculated from the captured images of the high-speed camera.

The selected projectile shape is a sphere, and the projectile material is carbon steel. The diameters of the spheres are (7 mm, 8 mm, and 10 mm). Table 1 shows the data of the sphere projectile. Figure 3 shows a schematic of the experimental apparatus for the ricochet test.

Table 1. Sphere projectiles

	Diameter	Density	Volume	Weight
Sphere	7 mm (±0.01)	7,500 kg/m <sup>3</sup> (±1.68)	179.59 mm <sup>3</sup> (±0.62)	1.40 g
	8 mm (±0.01)		268.08 mm <sup>3</sup> (±0.82)	2.09 g
	10 mm (±0.01)		523.59 mm <sup>3</sup> (±1.28)	4.08 g

In this study, a device for increasing the temperature of the sand was needed to investigate the effect of the sand temperature on the behaviour of the projectile. In order to heat the sand, an iron box was filled with sand, and heated. An iron box of shallow depth and large width was fabricated to heat the sand as uniformly as possible. The iron box with high heat conductivity was heated by a gas burner to raise the sand temperature. The dimensions of the iron box were 300 mm × 300 mm × 20 mm. Three thermocouples were inserted to a certain depth into the sand. Since the temperatures of all three of the thermocouples cannot be the same, the experiments were conducted when the sand temperatures at the three locations were similar.

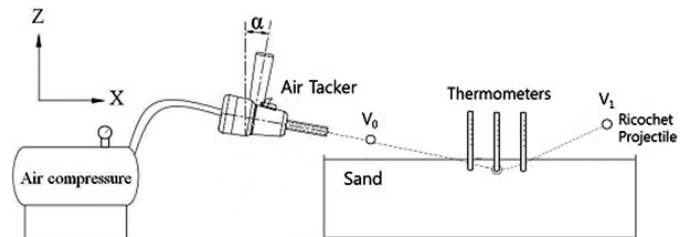


Figure 3. Experimental setup for ricochet.

### 3.3 The Procedure of the Vertical Launch Test

The diameters of the sphere selected for the vertical launch test were (5 mm and 7 mm). Two temperatures of the sand were selected: (20 °C and 100 °C). The pressure of the air compressor was set at 6 bar for all vertical launch tests. The vertical launch tests were carried out three times for each condition, and the following test procedure was applied:

- (i) The air pressure was controlled through the use of an air compressor to discharge the projectile.
- (ii) The launch device was adjusted so that the projectile was launched perpendicular to the sand surface.
- (iii) The sand was heated to the proper temperature for the test.
- (iv) The sand was removed after launch, and the penetration depth of the projectile was measured.

### 3.4 The Procedure of the Ricochet Test

In this study, the following four variables were selected: incident velocity, incident angle, sand temperature, and projectile diameter. The air pressures were (4 bar, 5 bar, and 6 bar) for the launch of the projectile, and the velocities were about (24 m/s, 28 m/s, and 32 m/s). The incident angles of the projectile were (15 °, 20 °, and 25 °). The sand temperatures were (20 °C, 50 °C, 80 °C, and 100 °C). The diameters of the sphere were (7 mm, 8 mm, and 10 mm). The ricochet tests were carried out three times for each condition, and the following test procedure was applied:

- (i) The air pressure was controlled through the use of an air compressor to discharge the projectile.
- (ii) The incident angle was adjusted by using the angle-control device of the air gun.
- (iii) The sand was heated to the proper temperature for the test.
- (iv) The heated sand was transferred to the ricochet test box, and the temperature of the sand was measured appropriately by using three thermometers. When the sand temperature was suitable for the tests, the test was conducted.
- (v) The projectile ricochet was recorded using the high-speed camera. The reflection angle and velocity of the projectile were calculated from the pictures that were taken by the camera.

## 4. FEM ANALYSIS

These days, building explosion research is conducted through FEM analysis, because of the cost, time and place to conduct experiments. Based on various theories, the initial conditions such as the incident velocity, incident angle and shape as well as the distance of the debris were predicted from the explosion of building by numerical analysis. In these studies, however, ricochet and rolling of debris were not considered to determine the debris ejection distance<sup>18-22</sup>. IBD research by building debris is also being studied through FEM<sup>23-25</sup>. For accurate FEM analysis, it is important to know the initial conditions, such as the shape, speed, and incident angle of the debris. However, it is important not only to consider the type of medium, but also to set precise physical properties according to the conditions of the medium, like temperature, void ratio,

internal friction angle, and water content. The dynamics analysis program does not allow the sand temperature to be input for any material, and even if the temperature can be set, the physical property corresponding to the temperature must be input. In this study, the shear stress and internal friction angle of sand were selected as factors influencing the penetration depth of a projectile when the temperature of sand increased. The two factors are input in place of the temperature change in the FEM analysis. Of these two factors, the internal friction angle was applied to the sand properties of the FEM analysis program. In other words, the sand temperature was replaced by the internal friction angle. The FEM analysis was carried out under the same condition as the ricochet experiment, and the effect of the internal friction angle on the ricochet of projectiles was analyzed. Through the FEM analysis, the kinetic energy loss rate of the projectile and the shear stress of the sand were analyzed in accordance with the internal friction angle.

## 4.1 FEM Modelling

### 4.1.1 Material Property of Steel

In this study, the projectile material was AISI 4340 steel. The density was 7,850 kg/m<sup>3</sup>, Poisson's ratio was 0.29, and the shear modulus was 74 x 10<sup>9</sup> Pa. Figure 4 shows the uniaxial stress-strain curve for AISI 4340 steel, whereby the strain rate changes rapidly at stress levels greater than 1,700 MPa<sup>26</sup>.

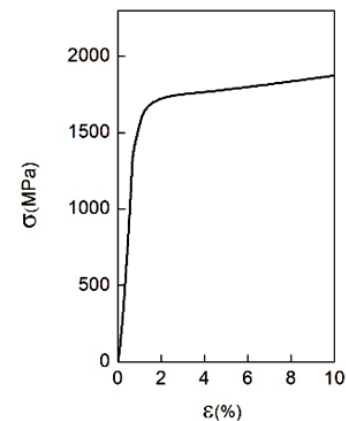


Figure 4. The uniaxial stress-strain curve for 4340 steel<sup>26</sup>.

### 4.1.2 Material Property of Sand

The sand density for the experiments was 1,500 kg/m<sup>3</sup>, and the shear modulus was  $G = 7.69 \times 10^7$  Pa. The coefficient of the friction of the sand and AISI 4340 steel was 0.35<sup>27</sup>. The sand-strength formula was set so that the tension strength was zero. The Mohr-Coulomb criterion setting was included in the cohesion effect. Figure 5 shows the MO granular-pressure hardening, wherein the three curves indicate the internal friction angle of the sand; these curves can be expressed by Eq. (3), as follows<sup>10</sup>:

$$\sigma_{ys} = \frac{\sigma_1 - \sigma_3}{2} = \begin{cases} P \cdot \tan \alpha & 0 < P < P_{mc} \\ P_{mc} \cdot \tan \alpha & P \geq P_{mc} \end{cases} \quad (3)$$

where  $\sigma_1$  and  $\sigma_3$  are the maximum and minimum stresses;  $\alpha$  is the internal-friction angle, which are 40°, 35°, and 30° for the three curves from the top;  $P$  is the pressure; and  $P_{mc}$  is the Mohr-Coulomb pressure. The property in the FEM analysis

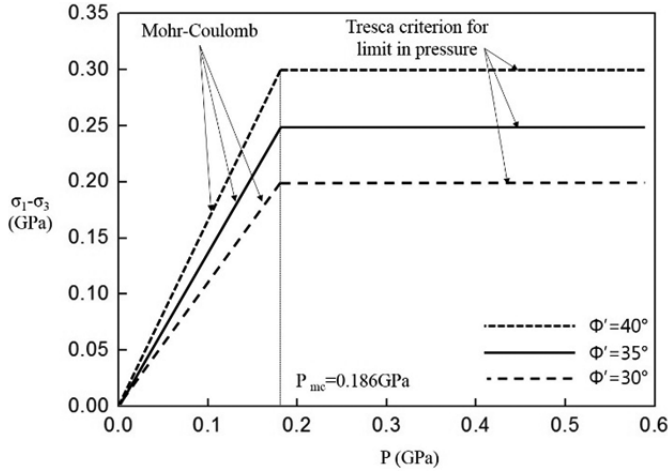


Figure 5. The Mohr-Coulomb criterion for internal friction angle.

that is affected by the sand temperature is the internal friction angle in Fig. 5. The pressure values for the internal friction angle of sand can be applied to the sand-material property in the FEM analysis. The internal friction angle was obtained by the direct shear test. The internal friction angles applied in this paper were 30° and 40°.

For the FEM analysis of the sphere projectile ricochet on sand, the dynamic-analysis program ANSYS Explicit Dynamics was used. The sand can be considered a continuum, because it is a fluid collection of small particles. Here, an arbitrary Lagrangian-Eulerian FEM was suitable for FEM analysis of the collision between the solid projectile and the sand; that is, the Lagrangian model was used for the solid, and the Euler model was used for the continuum<sup>28</sup>.

#### 4.1.3 Projectiles and Sand Modelling

All of the models of the projectile, sandbox, and sand that were used in the FEM were the same as those used in the experiments. Figure 6 shows the sphere, sandbox, and sand modeling of the FEM. A hexahedral mesh was selected for the sand, and the mesh size of 0.05 mm is similar to that of a real sand particle. The numbers of sand nodes and elements were 12,214,881 and 12,000,000, respectively.

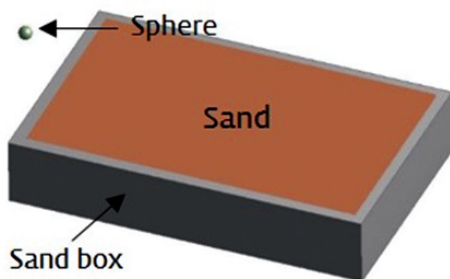


Figure 6. Sphere, sand, and sandbox modelling.

## 5. EXPERIMENTAL RESULTS

### 5.1 Direct Shear Test Results

A direct shear test was conducted to obtain the shear stress at three different sand temperatures. Figure 7 shows the shear strength of sand at the temperatures of 20 °C, 50 °C, and 100 °C.

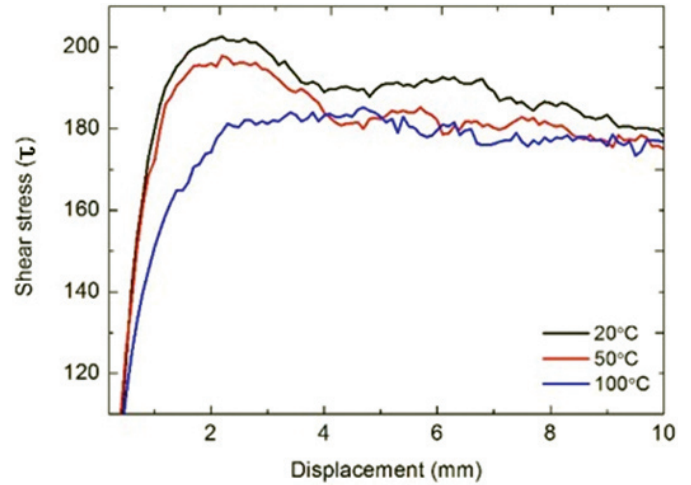


Figure 7. Sand direct-shear test at 20 °C, 50 °C, and 100 °C.

When the sand temperature is 20 °C, the maximum shear stress is greater than that for the 100 °C sand temperature. The shear stress of 50 °C is less than that of 20 °C, but they are similar. This shows that as the sand temperature increases, the shear stress of the sand decreases.

In the shear stress graph, the internal friction angle of the sand can be measured. This is because the shape of the graph changes depending on the internal friction angle. In the direct shear test conducted in this study, not only the stress, but also the shape of the graph changed. As the sand temperature increases, the peak of the graph descends down to the stress level similar to the final stress. This shows the change of sand density and internal friction angle. Figure 8 shows the sand density and internal friction angle according to the shape of the shear stress graph<sup>29</sup>. The figure shows that when the sand temperature changes from 20 °C to 100 °C, the density of the sand changes from dense to medium, and the friction angle of the sand drops from 38° to 30°. This means that the temperature change of the sand affects the shear stress and the internal friction angle of the sand.

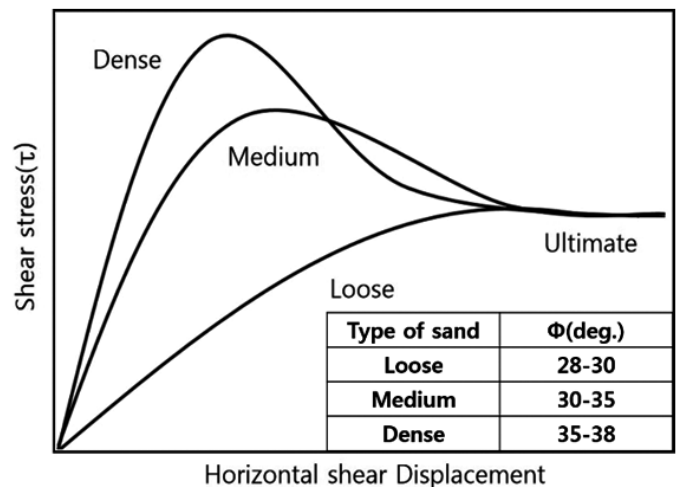


Figure 8. Results of direct-shear test in loose, medium, and dense sand, and the internal friction angle<sup>29</sup>.

**5.2 Vertical Launch Test Results**

Table 2 shows the penetration depths of the projectile when the projectiles were perpendicularly discharged to the sand for sand temperatures of 20 °C and 100 °C. The table shows that for higher sand temperature, the penetration depth is deeper. In the case of a 5 mm sphere, the penetration depth at 100 °C increased by 137.5 % compared to 20 °C, and increased by 120 % when the projectile was a 7 mm sphere. This implies that the temperature of the sand affects the penetration of the projectile.

**Table 2. Penetration depths of (5 and 7) mm spheres**

Diameter of Sphere projectile (mm)	Sand temp. (°C)	Penetration depth (mm)
5	20	40
	100	55
7	20	65
	100	78

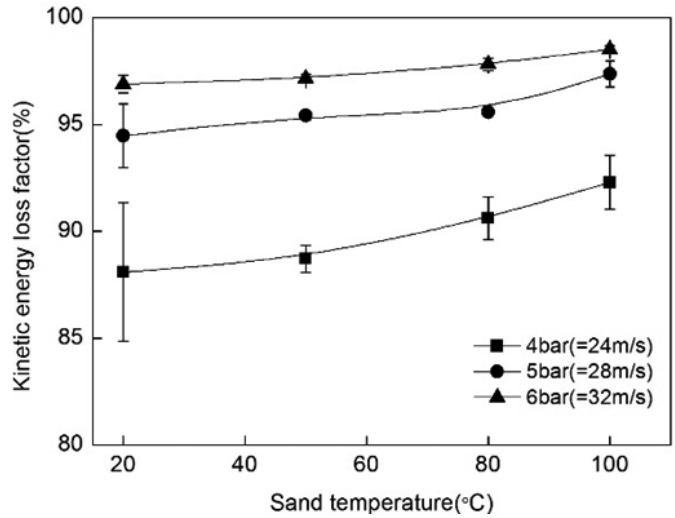
**5.3 Experimental Results**

This experiment was carried out to investigate the behaviour of the ricocheted projectile for different sand temperature. In order to obtain the effect of the sand temperature on the ricochet of the projectile, the kinetic energy loss rate of each projectile was used. This is because the speed of the projectile changes with the sand properties, which are affected by the sand temperature. A high kinetic energy loss rate means that the velocity of the ricocheted projectile is slower. A kinetic-energy loss factor is determined as follows. The incident velocity and the reflection velocity are denoted as  $V_0$  and  $V_1$ , respectively. The initial kinetic energy can be expressed as  $E_0 = 0.5 mV_0^2$ , where  $m$  is the projectile mass. Similarly, the reflection kinetic energy is  $E_1 = 0.5 mV_1^2$ . Hence, the kinetic-energy loss factor can be expressed as  $(1 - E_1/E_0) \times 100\%$ .

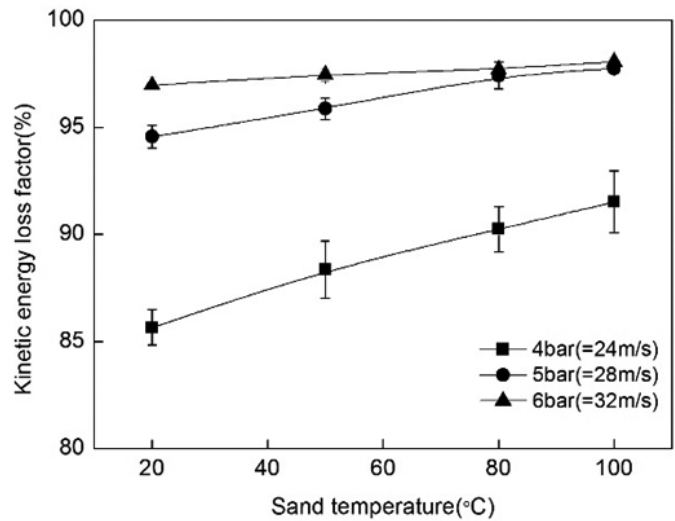
Figures 9-11 show the kinetic energy loss rate when the incident angle is 15°. Figure 9 shows the kinetic-energy loss factor of the 7 mm sphere after the ricochet when the incident angle is 15°, the air pressures are (4 bar, 5 bar, and 6 bar), and the sand temperatures are 20 °C, 50 °C, 80 °C, and 100 °C. The black squares indicate the average values of the kinetic-energy loss factor. When the sand temperature increases, the kinetic-energy loss factor also increases, and this means that the projectile velocity is lower than those of the low sand temperatures.

Figure 10 shows the kinetic-energy loss factors of the 8 mm sphere after the ricochet, when the incident angle is 15°, the air pressures are (4 bar, 5 bar, and 6 bar), and the sand temperatures are 20 °C, 50 °C, 80 °C, and 100 °C. The kinetic-energy loss factors increase with the increase of the sand temperature, and this means that the projectile velocity is lower than those of the low sand temperatures.

Figure 11 shows the kinetic-energy loss factors of the 10 mm sphere after the ricochet for air pressures of (4 bar, 5 bar, and 6 bar), and sand temperatures of 20 °C, 50 °C, 80 °C, and 100 °C. The kinetic-energy loss factor increases with the



**Figure 9. Kinetic-energy loss factor at 15° for 7 mm sphere.**



**Figure 10. Kinetic-energy loss factor at 15° for 8 mm sphere.**

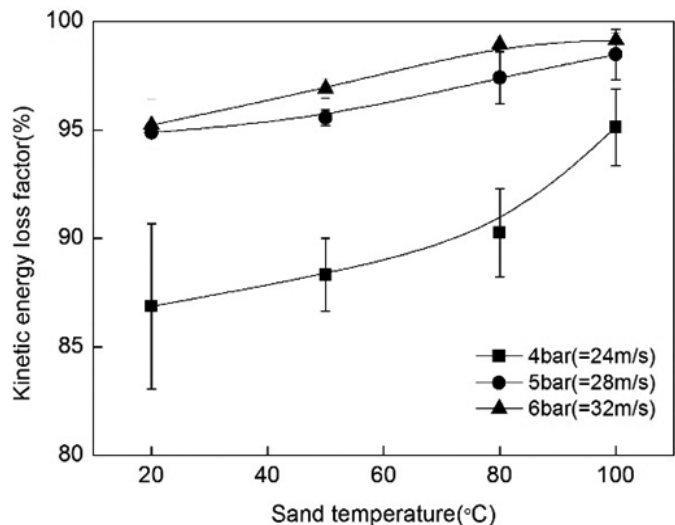


**Figure 11. Kinetic-energy loss factor at 15° for 10 mm sphere.**

increase of the sand temperature. When the sand temperature increases, the kinetic-energy loss factors increase at an incident angle of 15°.

Table 3 shows the difference in kinetic energy loss factor between 20 °C and 100 °C at ricochet test of (7 mm, 8 mm, and 10 mm) projectiles. The incident angle is 15°. The higher the discharge pressure, the lower the kinetic energy loss factor. As the diameter of the projectile decreases, the kinetic energy loss factor between the two temperatures decreases.

**Table 3. The difference in kinetic energy loss factor between (20 and 100) °C at 15° of incident angle**

	4 bar (%)	5 bar (%)	6 bar (%)
7 mm	4.2	2.9	1.63
8 mm	5.85	3.18	1.1
10 mm	8.26	3.61	4.91

The angle of incidence that best represents the effect of sand temperature is that at 20°. When the sand temperature was 20 °C, the projectile ricocheted in all conditions. However, when the sand temperature increased, projectiles did not ricochet. When the incident angle of the projectile was 25°, the projectile did not ricochet at all temperatures. This means that the critical angles of the spheres are about 25°.

**6. FEM RESULTS**

In this study, the shear stress according to sand temperature was measured, and the internal friction angle was determined from the shear stress graph. The assumptions made in this paper are as follows. As shown in Figs. 7 and 8, when the temperature of the sand is 20 °C, the internal friction angle is 40°. When the temperature of the sand is 100 °C, the internal friction angle is 30°. Assuming that the two conditions are the same, this was applied to the FEM analysis program. The internal friction angles were applied to the sand properties of the FEM analysis program. Therefore, the kinetic energy loss rate of the ricocheted projectile was calculated according to the change of the internal friction angle of the sand under the same conditions as the ricochet experiment. The shear stress that occurred when the projectile penetrates the sand were measured. There exists a relation between the shear stress and the internal friction angle.

Table 4 shows the kinetic energy loss rate of the projectile according to the internal friction angle, incident angle, and incident pressure. The rate of kinetic energy loss does not change much with the speed of the projectile, but when the internal friction angle increases, the kinetic energy loss rate decreases sharply. As the internal friction angle increases, the speed of the projectile decreases.

Table 5 shows the shear stresses generated in the sand when the projectile collides with the sand, depending upon the internal friction angle, the incident angle, and the incident pressure. Under all conditions, lower shear stress occurs when the internal friction angle is small.

**Table 4. Kinetic-energy loss factor for 10 mm sphere in FEM analysis: Incident angle at 15° and 20°**

Incident angle	at 15°			at 20°		
Internal friction angle	Air pressure					
	4 bar (%)	5 bar (%)	6 bar (%)	4 bar (%)	5 bar (%)	6 bar (%)
30°	84.85	84.48	83.78	99.24	98.83	98.61
40°	80.06	80.69	78.84	93.45	90.73	89.48

**Table 5. Shear stress of sand in FEM analysis: Internal friction angle at 40° and 30°**

Internal friction angle	at 40° (Mpa)			at 30° (Mpa)		
Incident angle	Air pressure					
	4 bar	5 bar	6 bar	4 bar	5 bar	6 bar
15°	0.321	0.082	0.296	0.200	0.033	0.256
20°	1.60	0.391	0.304	0.087	0.206	0.170
25°	0.247	0.493	1.915	0.088	0.068	0.782

**7. DISCUSSION**

In this study, the change of spherical projectile behaviour with sand temperature was studied. The changes in the physical properties due to the temperature change of the sand and its effect on the spherical projectile were examined. As the temperature of the sand increases, the penetration depth of the sphere projectile also increases. It is obvious that the sand temperature may play a key role in the ricochet. The change in depth of penetration implies a change in the resistance of the sand. To measure the resistance of the sand, the shear stress of the sand was measured through a direct shear test. As the temperature of the sand increases, the shear stress decreases. The change in the shear stress graph shape of the sand means change in the internal friction angle of the sand. As the temperature of the sand increases, the internal friction angle of the sand also decreases. These factors result in reducing the reflection velocity of the projectile, because increase in temperature causes a decrease in the shearing resistance at individual particle contacts. As a consequence, there is partial collapse of the sand structure and decrease in void ratio, until a sufficient number of additional bonds are formed to enable the sand to carry the stresses at high temperature<sup>29</sup>. This makes the penetration depth of the projectile deeper. At this time, since the surface area abutted against the medium becomes larger, more energy loss occurs. This is also the reason why ricochet is more likely to occur at low angles of incidence. This is because the penetration depths are not deep. As the penetration depth increases, the path of the projectile extends. Therefore, even when the projectile comes back to the surface of the medium, it experiences more energy loss. It can be seen from Table 3 that the projectile size affects the ricochet behaviour. When the projectile ricochets onto sand of higher temperature, the weight and the surface area increase, as the projectile diameter

increases. The kinetic energy of the penetrating projectile also increases. As a result, the projectile penetrates deeper into the sand. This makes a wider immersed area. Therefore, as the size of the projectile increases, the difference in kinetic energy loss factor at two temperatures increases, even when it is launched by the same pressure.

The shear stress and internal friction angle of the sand were selected as factors influencing the penetration depth of the projectile when the sand temperature increased. The FEM was used to investigate the effect of the internal frictional angle on the ricochet of the projectile. The factors determining the shear strength of sand are the effective stress, cohesion, and internal friction angle. The internal friction angle and shear strength of the sand are proportional<sup>15</sup>. As can be seen from the FEM analysis, the shear stress that is generated in the sand when the projectile is ricocheted is deeply related to the internal friction angle. The two relationships are proportional. As the internal friction angle increases, the shear stress that occurs also affects the behaviour of the projectile. As the internal friction angle increases, the shear stress that occurs also increases. This affects the behaviour of the projectile.

The sand temperature affects the shear stress and internal friction angle of the sand, and they affect the depth of the immersed edge of the sphere projectile, and change the behaviour of the projectile. When studying the behaviour of the projectile with FEM or other simulation, it is important to consider not only the projectile conditions, but also the conditions of the medium. The temperature of the sand cannot be considered in the FEM, but the internal friction angle suitable for each temperature can be obtained through experiments, to obtain the same tendency for the ricochet behaviour as in the actual experiment. The sand temperature and the internal friction angle are proportional to each other, and as the two increase, the kinetic energy loss factor of the projectile increases.

Table 4 compares the differences of the kinetic energy loss factors of the projectile at 20 °C and 100 °C, and the differences in the kinetic energy loss factor at 30° and 40° internal friction angle in the same ricochet experimental conditions with three incident pressures for 10 mm sphere projectile. The internal friction angle according to the sand temperature is applied to the FEM analysis, so that the results of the experiment and the FEM analysis can be compared. When the incident pressure is 4 bar, there is an error of 3.47 %. However, at the incident pressure of (5 bar and 6 bar), the error of the experiment and FEM analysis is very small. This means that the internal friction angle is well chosen for replacing the temperature. Also, this is why it is necessary to find the resistance of the medium through experiment, and apply it to the FEM analysis. If not applied, the FEM analysis will cause large errors in determining the IBD. However, the loss rate showed a slight difference in experiment and FEM analysis. This may result from the sand modeling in FEM. In this study, the sand is assumed to be a continuum. This is likely to have produced errors in the kinetic energy loss rate of the actual experiment and the FEM. In future work, the sand will be modeled in the FEM as a set of particles, rather than a continuum.

## 8. CONCLUSIONS

In this study, the ricochet of a sphere on sand was investigated experimentally and numerically for various sand temperatures and internal friction angle. The conclusions of this study are as follows:

- As the temperature of the sand increases, the shear stress and internal friction angle decrease. This affects the depth of the immersed edge of sphere. As the shear stress and the internal friction angle decrease, the resistivity of the sand decreases, so the depth of the immersed edge becomes deeper and the penetration trajectory in the sand increases. Therefore, the kinetic energy lost increases due to the friction and the speed of the ricocheted sphere decreases and the kinetic energy loss rate increases.
- In this study, it was confirmed in the analysis that the behaviour of the ricocheted sphere changes with the internal friction angle with temperature. This means that shear stress and internal friction angle, which vary with temperature, should be applied to the analysis to reduce the error of IBD in the debris ricochet study.

The results of this study can be used to determine a more-realistic IBD for the explosions that occur in areas that are mainly composed of hot, sand-like desert conditions; and it can also be used as a resource to select a safer place in emergency situations, in which there is falling debris from explosions.

## REFERENCES

1. Bocquet, L. The physics of stone skipping. *Am. J. Phys.*, 2003, **71**(2), 150–155.  
doi: 10.1119/1.1519232.
2. Johnson, W. Ricochet of non-spinning projectiles, mainly from water. Part I: Some historical contributions. *Int. J. Impact Eng.*, 1998, **21**(1–2), 15–24.  
doi: 10.1016/S0734-743X(97)00032-8.
3. Johnson, W. Ricochet of spinning and non-spinning spherical projectiles, mainly from water. Part II: An outline of theory and warlike applications. *Int. J. Impact Eng.*, 1998, **21**(1–2), 25–34.  
doi: 10.1016/S0734-743X(97)00033-X.
4. Johnson, W. & Reid, S.R. Ricochet of spheres off water. *J. Mech. Eng. Sci.*, 1975, **17**(2), 71–81.
5. Daneshi, G.H.; Johnson, W. The ricochet of spherical projectiles off sand. *Int. J. Mech. Sci.*, 1977, **19**(8), 491–497.
6. Bai, Y.L. & Johnson, W. The effects of projectile speed and medium resistance in ricochet off sand. *J. Mech. Eng. Sci.*, 1981, **23**(2), 69–75.  
doi: 10.1243/JMES\_JOUR\_1981\_023\_015\_02.
7. Johnson, W. & Daneshi, G.H. The trajectory of a projectile when fired parallel and near to the free surface of a plastic solid. *Int. J. Mech. Sci.*, 1978, **20**(4), 255–263.  
doi: 10.1016/0020-7403(78)90087-5.
8. Sundararajan, G. & Shewmon, P.G. The oblique impact of a hard ball against ductile, semi-infinite target materials-experiment and analysis. *Int. J. Impact Eng.*, 1987, **6**(1), 3–22.  
doi: 10.1016/0734-743X(87)90003-0.
9. Knock, C.; Horsfall, I.; Champion, S.M. & Harrod, I.C.

- The bounce and roll of masonry debris. *Int. J. Impact Eng.*, 2004, **30**(1), 1–16.  
doi: 10.1016/S0734-743X(03)00057-5.
10. Xu, J.; Lee, C.K.; Fan, S.C. & Kang, K.W. A study on the ricochet of concrete debris on sand. *Int. J. Impact Eng.*, 2014, **65**, 56–68.  
doi: 10.1016/j.ijimpeng.2013.11.003.
  11. Xu, J.; Lee, C.K. & Fan, S.C. A Study on the Ricochet of concrete debris against soil. *Int. J. Comput. Methods*, 2015, **12**(4), 1540009.  
doi: 10.1142/S0219876215400095.
  12. Fan, S.C.; Lee, C.K.; Kang, K.W. & Wu, Z.J. Validation of a flight model for predicting debris trajectory from the explosion of an ammunition storage magazine. *J. Wind Eng. Ind. Aerodyn.*, 2015, **136**, 114–126.  
doi: 10.1016/j.jweia.2014.11.004.
  13. Ferris, G.W. An elastic plastic approach, modeling deformation of dense sand. University of Manitoba, Winnipeg, Canada, 2000, Master thesis.
  14. Graham, J.; Alfaro, M.; Ferris, G. Compression and strength of dense sand at high pressures and elevated temperatures. *Can. Geotech. J.*, 2004, **41**(6), 1206–1212.  
doi: 10.1139/t04-047.
  15. Das, Braja M. Advanced soil mechanics (Fourth edition). CRC Press, 2014.
  16. Nicholson, Sharon E. Dryland climatology. Cambridge University Press: 2011.
  17. De Podesta, M. Bouncing steel balls on water. *Phys. Educ.*, 2007, **42**(5), 466–477.  
doi: 10.1088/0031-9120/42/5/003.
  18. Lu, Y. & Xu, K. Prediction of debris launch velocity of vented concrete structures under internal blast. *Int. J. Impact Eng.*, 2007, **34**(11), 1753–1767.  
doi: 10.1016/j.ijimpeng.2006.09.096.
  19. Wang, M.; Hao, H.; Ding, Y. & Li, Z.X. Prediction of fragment size and ejection distance of masonry wall under blast load using homogenized masonry material properties. *Int. J. Impact Eng.*, 2009, **36**(6), 808–820.  
doi: 10.1016/j.ijimpeng.2008.11.012.
  20. Van Der Voort, M.M. & Weerheijm, J. A statistical description of explosion produced debris dispersion. *Int. J. Impact Eng.*, 2013, **59**, 29–37.  
doi: 10.1016/j.ijimpeng.2013.03.002.
  21. Keys, R.A. & Clubley, S.K. Establishing a predictive method for blast induced masonry debris distribution using experimental and numerical methods. *Eng. Fail. Anal.*, 2017, pp. 1-19.  
doi: 10.1016/j.engfailanal.2017.07.017.
  22. Wei, J.F.; Zhang, C. & Wang, S.S. Detonation output properties of D-shape structure. *Def. Sci. J.*, 2014, **64**(5), 471–476.  
doi: 10.14429/dsj.64.4746.
  23. Lim, H. S.; Kang, K. W.; Fan, S. C.; Yu, Q. J. & Yang, Y. A review: Numerical modeling of the debris throw of reinforced concrete structures under internal explosions. 34th DoD Explosive Safety Seminar, Portland, Oregon, 2010.
  24. Xu, J.; Lee, C.K. & Fan, S.C. Numerical modeling on concrete debris ricocheting off sand ground. APCOM & ISCM, Singapore, 2013.
  25. Fan, S. C.; Yu, Q. J.; Yang, Y.; Lim, H. S. & Kang, K. W. Study of debris throw and dispersion after break-up of reinforced concrete structure under internal explosion. 34th DoD Explosive Safety Seminar, Portland, Oregon, 2010.
  26. Premack, T. & Douglas, A.S. Three-dimensional analysis of the impact fracture of 4340 steel. *Int. J. Solids Struct.*, 1995, **32**(17-18), 2793–2812.  
doi: 10.1016/0020-7683(94)00295-8.
  27. Leonards, G.A. Experimental study of static and dynamic friction between soil and typical construction materials. User report No. AFWL-TR-65-161. April 1965.
  28. Donea, J.; Huerta, A.; Ponthot, J.-P. & Rodríguez-Ferran, A. Arbitrary Lagrangian-Eulerian Methods. *Encycl. Comput. Mech.*, 2004, (1969), 413–437.  
doi: 10.1002/0470091355.ecm009.
  29. James K. Mitchell & Soga, K. Fundamentals of soil behavior. Third John Wiley & Sons, Inc., 2005.

#### ACKNOWLEDGMENTS

This study was financially supported by the Foundation Research Program under contract No. UD170027GD through the Agency for Defense Development grant funded by the Defense Acquisition Program Administration.

#### CONTRIBUTORS

**Mr Yoon Keon Kim**, received his BS (Mechanical Engineering) from Myongji University, Republic of Korea. He is currently pursuing his PhD from Korea University at Precision Technology Laboratory, Seoul, Republic of Korea. His areas of interests are ricochet phenomenon of debris and projectile onto various medium, projectile penetration in sand, and FEM analysis for ricochet and penetration.

In the present study, his contributions are in the design of the experiments, implementation of experiments, FEM analysis and he wrote the manuscript.

**Dr Woo Chun Choi**, received his BS and MS in Mechanical Engineering from Seoul National University, Republic of Korea, in 1982 and 1984, respectively. He obtained his PhD (Mechanical Engineering) from MIT in 1990. He is presently working as Professor at Department of Mechanical Engineering in Korea University, Republic of Korea. His research area includes precision engineering, and manufacturing processes.

In the present study, he contributed to provide the overall guidance and reviewed the manuscript.